

Document downloaded from:

<http://hdl.handle.net/10251/195000>

This paper must be cited as:

Arenhart-Heberle, AN.; Vianna, GGF.; Da Silva, SW.; Pérez-Herranz, V.; Moura Bernardes, A. (2022). Evaluation of an electrochemical membrane reactor for the removal of beta-blocker compound from water. *Journal of Water Process Engineering*. 47:1-9.
<https://doi.org/10.1016/j.jwpe.2022.102830>



The final publication is available at

<https://doi.org/10.1016/j.jwpe.2022.102830>

Copyright Elsevier

Additional Information

Evaluation of an electrochemical membrane reactor for the removal of β -blocker compound from water

Alan Nelson Arenhart Heberle^{a,c}, Giulia Grimaldi Falavigna Vianna^a, Salatiel Wohlmuth da Silva^{b*}, Valentín Pérez-Herranz^c, Andréa Moura Bernardes^a

^a Universidade Federal do Rio Grande do Sul (UFRGS) – Programa de Pós-Graduação em Engenharia de Minas, Metalúrgica e de Materiais (PPGE3M), Av. Bento Gonçalves, 9500, Porto Alegre, RS, Brazil.

^b UFRGS, Instituto de Pesquisas Hidráulicas (IPH) – Programa de Pós-Graduação em Recursos Hídricos e Saneamento Ambiental, Av. Bento Gonçalves, 9500, Porto Alegre, RS, Brazil.

^c Grupo IEC, Departamento de Ingeniería Química y Nuclear, E.T.S.I. Industriales, Universitat Politècnica de València (UPV), P.O. Box 22012, E-46071, Valencia, Spain.

*Corresponding author: salatiel.silva@ufrgs.br

ABSTRACT

As part of the Brazilian Popular Pharmacy Program, the β -blocker Atenolol (ATN) is widely used, and its presence in the environmental ecosystems is a reality. Aiming the ATN removal, the use of an electrochemical membrane reactor was evaluated and compared to a membraneless one. The results show that the generation of $\text{SO}_4^{\bullet-}$ in the membrane reactor occurs by the reaction of $\text{HSO}_4^-/\text{H}_2\text{SO}_4$ scavenging HO^\bullet , whereas, in the membraneless reactor, the $\text{SO}_4^{\bullet-}$ generation occurs mainly by the direct oxidation mechanism. Operating both reactors in the same hydrodynamic conditions, it was found that the concentrations of $\text{SO}_4^{\bullet-}$ and $\text{S}_2\text{O}_8^{2-}$ are higher in the membrane reactor, leading to a greater concentration of these species being transported to the bulk solution, changing the kinetics, and presenting better results in electrochemical combustion (ϕ), mineralization current efficiency (MCE) and specific energy consumption (E_s). Since the mass transport limitations were overcome in membrane reactor, the processes may find their good applications in water and wastewater treatment.

KEYWORDS: Membrane reactor; electrochemical oxidation; β -blocker atenolol; Nb/BDD; oxidants generation.

1 INTRODUCTION

The unknown effects of long-term exposure to emerging organic micropollutants (EOM) have attracted attention in recent years [1]. There are evidences to suggest that the causes of some diseases, behavior changes, and endocrine disorders could be attributed to the exposition to these compounds [2–4]. Besides that, most of the studies assess acute rather chronic effects [5]. The EOM can be found in soil [6], air [7] and water, but in the aquatic environment they often accumulate, harming intensely human and wild life [8,9]. Furthermore, EOM are daily household used, such as some cleaning and personal care products, surfactants, hormones and pharmaceuticals [10,11].

The main environmental inlet of the EOM are the conventional wastewater treatment plants, since they are not designed to remove effectively such micropollutants [4,9,12]. Widely consumed substances, as pharmaceuticals, are consequently worldwide discharged into the environment, being detected in the water from many countries [13]. The β -blockers, such as Atenolol (ATN), are often applied in the treatment of the cardiocirculatory system diseases [14]. In fact, ATN was the fourth best-selling drug in Brazil, because it is part of the Brazilian Popular Pharmacy Program. The program aims to reduce the price of essential drugs through government subsidies [15]. Due to the high consumption, ATN was detected in hospital wastewater [16] and water sources in the city of Porto Alegre – Brazil [17], being also detected in wastewaters from other countries [13,18,19].

A work conducted by Vieno et al. [20] demonstrated that ATN presents toxicity for aquatic animals and humans. Considering that, effective processes should be developed, or the already existed methodologies should be improved, to thoroughly remove such micropollutants from water.

Electrochemical advanced oxidation processes (EAOPs) are methodologies that are able to promote EOM abatement [21–23] due to the generation of hydroxyl radical (HO^\bullet). Among the EAOP, we can highlight the electrochemical oxidation (EO) process, as it is a versatile, easy to operate and to scale-up.

The EO mechanism employ direct and/or indirect oxidation [24]. For direct oxidation, the micropollutant changes electrons directly with the anode surface, whereas in the indirect oxidation, the degradation is mediated by the active generated species, mainly the HO^\bullet [25].

In the EO process the direct and the indirect oxidation by HO^\bullet occurs at the anode surface, meaning that the EO process will be limited by the transport of the micropollutant from the bulk solution to the anode

surface, which can be considered a disadvantage of the process. Nevertheless, depending on the electrode material and supporting electrolyte, sulfate radical ($\text{SO}_4^{\cdot-}$) and persulfate ions ($\text{S}_2\text{O}_8^{2-}$) can be generated [26–28]. Sulfate species are not chemically/physically adsorbed on the anode surface and $\text{SO}_4^{\cdot-}$ have longer half-life time (30 - 40 μs) than HO^{\cdot} ($< 1 \mu\text{s}$) [29], being able to flow freely in the bulk solution [24,30,31], overcoming the mass transport limitation and playing an important role in the degradation and mineralization of the micropollutants.

The boron-doped diamond (BDD) anode presents some advantages over other materials, such as wide potential window, high current efficiency and high electrochemical and corrosion stability [32]. Over last years, BDD over niobium substrate (Nb/BDD) in a single compartment reactor have been effectively used to the degradation of pharmaceuticals [27,33,34], dyes [35], pesticides [36], hormones [37] and oil refinery effluents [38,39].

Although the degradation viability of EOM by the EO process have been proved [40,41], the implementation process and reactor design to favor effective generation of oxidation species, and to overcome mass transport limitations, is still a subject of study [42]. The oxidation of organic compounds can be more efficient when the anodic and cathodic reactions take place in separated compartments by ion exchange membranes [43].

The main goal of this work was to evaluate an electrochemical membrane reactor for the removal of the β -blocker ATN from water. For that, a cationic Nafion[®] – 117 membrane was employed in the electrochemical reactor, which was operated with different applied current densities (j_{app}) and sodium sulfate concentrations. The results were evaluated in terms of ATN degradation, mineralization and kinetics. Besides that, electrochemical combustion (ϕ), mineralization current efficiency (MCE) and specific energy consumption (E_s), were also evaluated and compared to the electrochemical process without membrane. In addition, the ATN direct and/or indirect oxidation mechanism and the main pathway for the generation of oxidants were studied by linear sweep voltammetry (LSV) and scavenging tests.

2 METHODS

2.1 Materials and reagents

Acetonitrile and phosphoric acid of HPLC grade were supplied by Supelco. The β -blocker Atenolol ($\geq 98\%$) was purchased from Sigma-Aldrich. Sodium sulfate (99.0%), tert-butanol (TBA, $\geq 99.0\%$) and ethanol (EtOH, $\geq 99.0\%$) were supplied by Neoquímica.

All standard solutions were prepared with ultrapure water (18.2 M Ω cm) from a Direct-Q UV (Millipore) water purification system. The work solutions were prepared using deionized and distilled water (1.9 μ S, pH 6.6 and 25°C).

The Nb/BDD₂₅₀₀ anode, doped with 2500 mg kg⁻¹ of Boron, was purchased from NeoCoat[®], and the cathode was a stainless steel AISI 304 L kindly provided by Bruning Tecnometal. A cationic Nafion[®] – 117 membrane was supplied by Sigma-Aldrich. Both electrodes and membrane are square, with a geometric surface area (A_g) of 0.01 m².

The Seaflo 686 pumps were purchased from Seaflo and the DC power supply (FCCT 150-15-i32110) was supplied by Supplier.

2.2 Solutions

The anodic solution was prepared by dissolving ATN in deionized and distilled water to a final concentration of 0.38 mM. After that, it was added 14, 28 or 56 mM of Na₂SO₄ as supporting electrolyte. The cathodic solution was prepared diluting 500 mM of the supporting electrolyte in deionized and distilled water.

2.3 Electrochemical oxidation

ATN oxidation assays were performed on a double compartment filter-press membrane reactor (DCMR) (**Error! No se encuentra el origen de la referencia.**). The reactor compartments have the same volume (0.3 L), and a cationic membrane was used to separate them. The flat square electrodes were positioned in parallel with a gap of 6 cm between them. One liter (1 L) of the anodic solution was stored in an external anodic reservoir and circulated through the anodic compartment by a centrifugal pump with a flow rate of $1.67 \times 10^{-5} \text{ m}^3 \text{ s}^{-1}$ (Fig. 1b). The same procedure was performed for the cathodic solution. Electrochemical oxidation was conducted in galvanostatic mode applying a current density (j_{app}) of 5, 10, 20, 30 or 40 mA cm⁻².

². To compare the results, assays were conducted in the same way as above mentioned, but without the membrane.

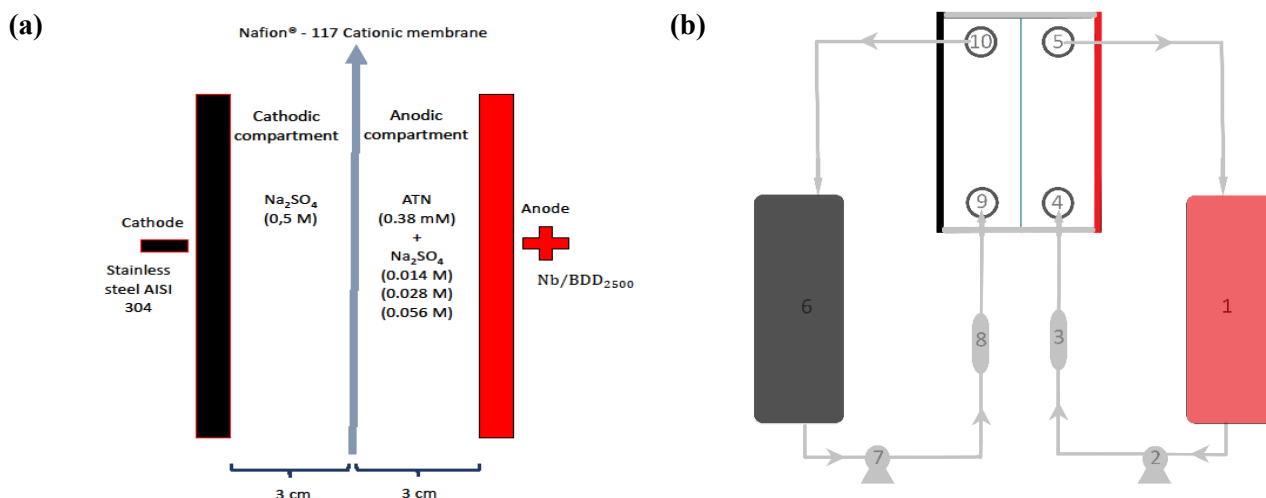


Fig. 1. (a) Detailed scheme of the proposed DCMR for the ATN oxidation at Nb/BDD₂₅₀₀ anode with different Na₂SO₄ concentrations and distinct current densities. (b) is the proposed operational system, where (1) is the external anodic solution reservoir, (2) is the anodic solution centrifuge pump, (3) is the anodic solution rotameter, (4) is the reactor anodic solution inlet, (5) is the reactor anodic solution outlet, (6) is the external cathodic solution reservoir, (7) is the cathodic solution centrifuge pump, (8) is the cathodic solution rotameter, (9) is the reactor cathodic solution inlet and (10) is the reactor cathodic solution outlet.

2.3.1 Characterization of the reaction mechanisms in DCMR

Aiming to characterize the ATN reaction mechanisms in the EO using the membrane reactor, linear sweep voltammetry (LSV) was conducted with three-electrodes in the anodic compartment of the cell divided by the cationic membrane Nafion® – 117. The working electrode was Nb/BDD₂₅₀₀, Pt was the counter electrode and saturated Ag/AgCl was used as reference electrode. All LSV were recorded in the anodic compartment at a scan rate of 5 mV s⁻¹ and a step potential of 0.45 mV by using a potentiostat/galvanostat Autolab model PGCTAT 302N controlled by a computer.

To corroborate with the aforementioned, and identify the radical species formed in the anodic compartment of DCMR (Fig. 1), and their influence on ATN removal, scavenging test were conducted with the addition of excess of TBA and EtOH. The TBA was employed as HO• scavenger, while EtOH was used as SO₄^{•-} scavenger [44]. This choice can be linked to the fact that the reaction rate of SO₄^{•-} with TBA

($4 - 9.1 \times 10^5 \text{ M}^{-1} \text{ s}^{-1}$) is slower than that with EtOH ($1.6 - 7.7 \times 10^8 \text{ M}^{-1} \text{ s}^{-1}$). On the other hand, HO^\bullet reacts faster than $\text{SO}_4^{\bullet-}$ both with EtOH ($1.2 - 2.8 \times 10^9 \text{ M}^{-1} \text{ s}^{-1}$) and with TBA ($3.8 - 7.6 \times 10^8 \text{ M}^{-1} \text{ s}^{-1}$). The concentrations of the scavengers (1 and 2 M of the TBA and EtOH, respectively), were those indicated to provide the scavenger and the preferably reaction to the radical, as proposed by the literature [45,46].

2.4 Analyses

At a given time, samples were collected and stored. After that, triplicate stored samples were transformed in composite sampling and submitted to different analytical methods.

ATN degradation and carboxylic acids generation were monitored by high performance liquid chromatography (HPLC) with a Shimadzu LC20A apparatus with a diode array detector (DAD) SPD-20AV and an auto-sampler SIL-20A. In both cases, 20 μL of the sample were injected.

For ATN decay analysis, the equipment was fitted with a Shim-pack XR-ODS C18 (3.0 mm ID \times 50 mm, Shimadzu) column. A 0.025 M phosphate buffer (pH 2.5) and acetonitrile were respectively used as mobile phase-A and mobile phase-B. The analyses were performed in isocratic mode, with 30 % of the mobile phase-A and 70 % of the mobile phase-B at a flow rate of 1.0 mL min^{-1} and the DAD set in $\lambda = 225 \text{ nm}$. In these conditions, the ATN retention time was 3.1 min.

On the other hand, the detection of carboxylic acids was performed using 50 mM of H_2SO_4 as mobile phase and an ion-exclusion (Rezex Roa-Organic acid H^+ column 8 %, $100 \times 4.6 \text{ mm}$, Phenomenex) as stationary phase. The detector was set in $\lambda = 210 \text{ nm}$ and the running was performed at a flow rate of 0.1 mL min^{-1} . The retention times of the carboxylic acids under these conditions were: oxalic (6.16 min), tartaric (7.78 min), formic (11.65 min), acetic (12.65 min), propionic (14.75 min) and isovaleric (20.82 min).

The mineralization was verified by the total organic carbon (TOC) analysis, with Non-Purgeable Organic Carbon (NPOC) method in a TOC-L CPH Shimadzu, following the instructions of the TOC Shimadzu manual.

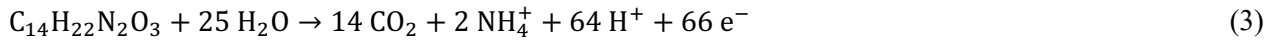
Based on degradation and mineralization results, the extent of electrochemical combustion (ϕ), can be estimated by the equation (1) [47].

$$\phi = \frac{\% \text{TOC}_{\text{removed}}}{\% \text{ATN}_{\text{removed}}} \quad (1)$$

The mineralization current efficiency (MCE, %) was estimated by Eq. 2 [48].

$$\text{MCE (\%)} = \frac{n \cdot F \cdot V \cdot (\text{TOC}_0 - \text{TOC})}{7.2 \cdot 10^5 \cdot m \cdot I \cdot t} \cdot 100 \quad (2)$$

where n is the number of exchanged electrons (66), F is the Faraday constant ($96,500 \text{ A s}^{-1} \text{ mol}^{-1}$), V is the total volume of the anodic solution (L), TOC_0 and TOC are the TOC concentrations (mg C L^{-1}) of the anodic solution at the beginning of the electrolysis and at each studied time, respectively, 7.2×10^5 is a conversion factor ($60 \text{ s min}^{-1} 12000 \text{ mg mol}^{-1}$), m is the number of carbon atoms of each ATN molecule (14), I is the applied current (A) and t is the time in minutes. It was assumed that 66 electrons were consumed overall, and that the mineralization involves the release of NH_4^+ ions according to the Eq. 3 [49].



The specific energy consumption (E_s , kW h kg^{-1}) was estimated by Eq. 4 adapted from García-Gabaldón et al., [50].

$$E_s = 16.66 \cdot \frac{U \cdot I \cdot t}{V \cdot (\text{TOC}_0 - \text{TOC})} \quad (4)$$

where 16.66 is a conversion factor ($\text{h } 60 \text{ min}^{-1} \text{ mg g}^{-1}$) and U in volts is the cell potential.

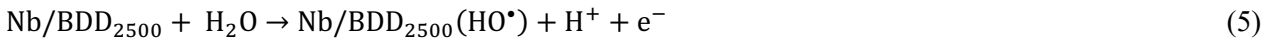
The pH was monitored by a potentiometric method by a Digimed DM-22.

3 RESULTS AND DISCUSSION

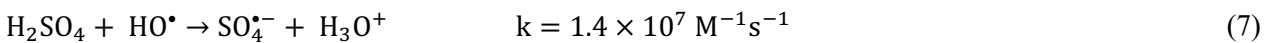
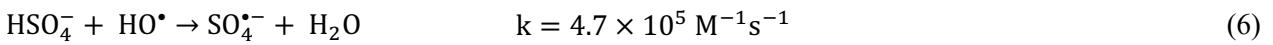
3.1.1 Reaction mechanisms in DCMR

The nature of the anode material, the j_{app} and Na_2SO_4 concentration can influence the oxidant species generated and the main oxidation mechanism [51]. Aiming to elucidate that, LSV containing the studied concentrations of Na_2SO_4 , with and without ATN, were performed in acid pH, which was chosen because. after EO process starts, using a cationic membrane, there will be a disbalance of protons in the compartments, leading to an acidification in the anodic compartment and an alkalinization in the cathodic one, reaching values near to 1.5 and 11, respectively.

It is observed in Fig. 2a that a high potential for oxygen evolution reaction (OER) was found, meaning that the anode has a high diamond- sp^3 content. This characteristic can favor the generation of HO^\bullet due to water splitting (Eq. 5). Nevertheless, knowing that the addition of Boron in the diamond layer leads to the generation of carbon- sp^2 impurities, and that carbon- sp^2 have higher adsorption capacity than diamond- sp^3 , direct oxidation and the generation of $\text{SO}_4^{\bullet-}$ and $\text{S}_2\text{O}_8^{2-}$ can also occur.



The $\text{SO}_4^{\bullet-}$ generation can be driven basically by two mechanisms, direct and/or indirect, depending on the anode, supporting electrolyte, j_{app} and pH characteristic. The indirect mechanism is described in Eqs. 6 - 7, where HSO_4^- and/or H_2SO_4 will react with the HO^\bullet , resulting in sulfate radical ($\text{SO}_4^{\bullet-}$) [52,53]. In the direct mechanism, sulfate will interact directly with the sp^2 -carbon impurities to generate $\text{SO}_4^{\bullet-}$ [53]. After electrogeneration, the $\text{SO}_4^{\bullet-}$ react in pairs, giving $\text{S}_2\text{O}_8^{2-}$, as shown in Eq. (8) [52].



A work conducted by Santos et al. [54] demonstrated by LSV that if the $\text{SO}_4^{\bullet-}$ formation occurs via direct and indirect oxidation, two slopes in the Tafel plots will appear: one between 1 - 1.5 V vs. Ag/AgCl and another between ~2.25 - 2.55 vs. Ag/AgCl, respectively. Observing Fig. 2a it is noted only one slope near to ~2.25 - 2.55 vs. Ag/AgCl, associated to the indirect generation of sulfate to $\text{SO}_4^{\bullet-}$ by Eqs. 6 - 7, meaning that the indirect path will be responsible to generate $\text{SO}_4^{\bullet-}$ at the membrane reactor. This fact can be attributed

to sulfate speciation and chemical equilibrium diagrams (Fig. S1, supplementary material). At acid pH, that is the case of the anodic compartment of the membrane reactor, the predominant species will be HSO_4^- and H_2SO_4 , facilitating the indirect electrochemical generation of $\text{SO}_4^{\bullet-}$.

After the addition of ATN in the media (Fig. 2b and insert graphic), it is noted peaks characteristics of the direct oxidation of the ATN. In this case, ATN will be oxidized by direct electron transfer and indirect oxidation by HO^\bullet , $\text{SO}_4^{\bullet-}$ and $\text{S}_2\text{O}_8^{2-}$ in the membrane electrochemical reactor.

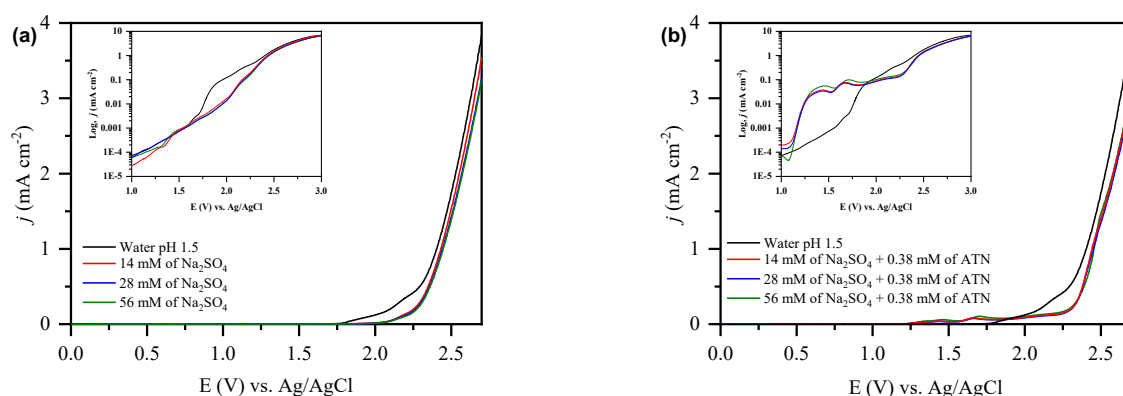


Fig. 2. LSV curves recorded in water at pH of 1.5 at a scan rate of 5 mV s^{-1} . **(a)** with and without supporting electrolyte and **(b)** with and without supporting electrolyte and ATN. The inset is the Tafel plots.

To confirm the findings described above, specific radical scavenger experiments were conducted. Fig. 3 shows that the scavenging effect on degradation of ATN in the presence of 1 M TBA was similar to those found in the presence of 2 M EtOH, meaning that the $\text{SO}_4^{\bullet-}$ was electrochemically generated through reactions 6 and 7. These findings demonstrate that HO^\bullet , presenting better oxidizing ability than $\text{SO}_4^{\bullet-}$ in acid pH, could react with HSO_4^- or/and H_2SO_4 to generate $\text{SO}_4^{\bullet-}$ and, by two molecule recombination, $\text{S}_2\text{O}_8^{2-}$ (Eq. 8). In this case, sulfate might play an important HO^\bullet scavenger, and, depending to the electrolysis condition (supporting electrolyte concentration and j_{app}), will affect the ATN degradation and mineralization rate.

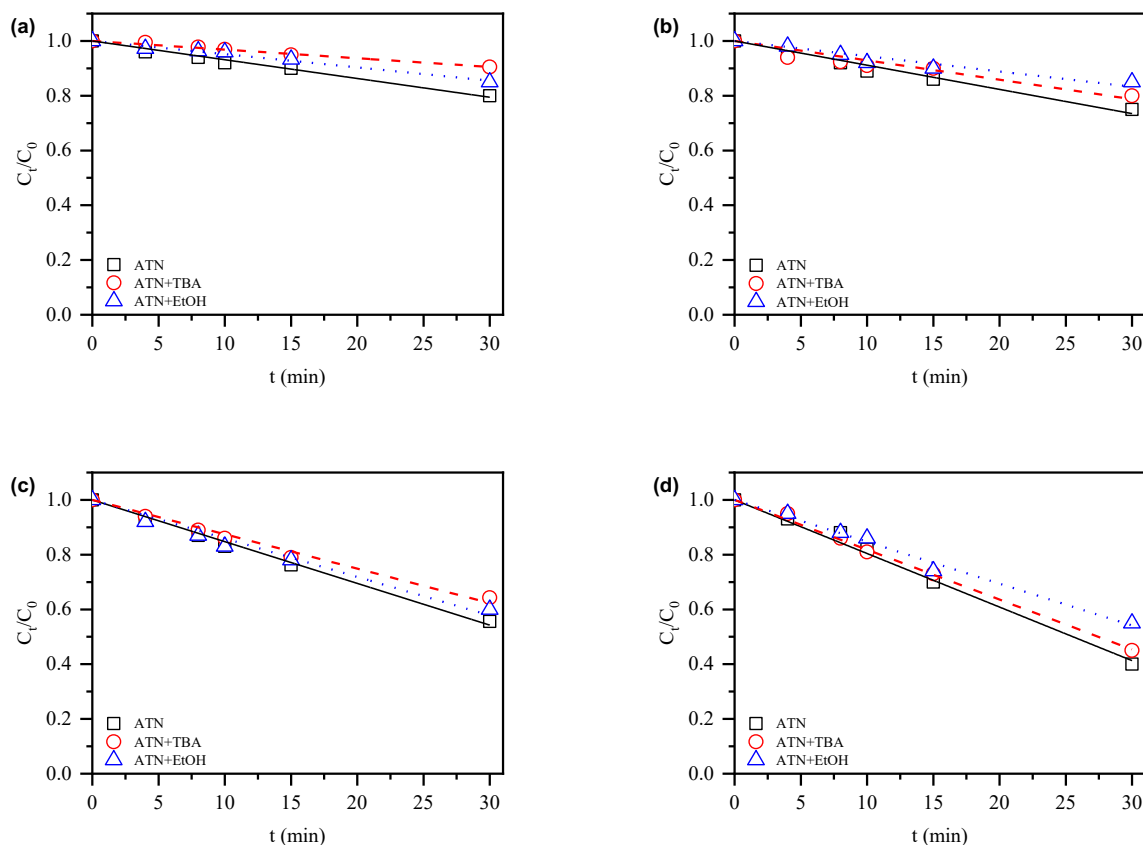


Fig. 3. Influence of the scavenger presence (1 M of TBA or 2 M Ethanol) in the degradation of 0.38 mM of ATN in acid pH using DCMR: (a) 0.014 M of Na_2SO_4 and 5 mA cm^{-2} , (b) 0.056 M of Na_2SO_4 and 5 mA cm^{-2} , (c) 0.014 M of Na_2SO_4 and 40 mA cm^{-2} , (d) 0.056 M of Na_2SO_4 and 40 mA cm^{-2} .

3.1.2 Effect of operating parameters on the oxidation of ATN in DCMR

The j_{app} and electrolyte are considered as the key factor in all EAOPs, the first can be easily and directly controlled, and the second one increases the conductivity of the solutions [51]. Besides that, the choice of electrolyte and the j_{app} can also influence the electrogeneration of oxidants species [55]. For that, experiments were conducted to analyze the influence of the j_{app} and Na_2SO_4 concentration on the ATN degradation (Fig. 4a, 4b and 4c) and mineralization (Fig. 4d, 4e and 4f) using the DCMR.

As j_{app} rises from 5 to 40 mA cm^{-2} an increase in the ATN degradation and mineralization can be observed, probably due to the higher generation of oxidants like HO^\bullet , $\text{SO}_4^{\bullet-}$, $\text{S}_2\text{O}_8^{2-}$, and direct oxidation also occurs, as proved in Fig. 2. This finding agrees with the literature, where it is shown that, in general, by increasing the j_{app} there will be an increase in the oxidation rate of organics [33,56]. However, mineralization

current efficiency tends to decrease, while energetic consumption will increase due to parallel oxygen evolution reactions [57].

It is also observed that for all j_{app} , the results show an exponential ATN oxidation decay, indicating that the EO are under mass transport control. Nevertheless, previous results using a single compartment reactor showed that for j_{app} between 5 and 20 mA cm⁻², the electrochemical process was controlled by the applied current [41]. Taking the difference for low current densities into consideration, and assuming that the hydrodynamic conditions are equal, the results indicated that the main corresponding oxidation mechanisms are different in DCMR. In this case, as a strong acid condition prevails in the anodic compartment, the main species will be HSO₄⁻ (Fig. S1 in supplementary material), that via indirect oxidation will scavenge HO• to generate SO₄^{•-}, and after that two SO₄^{•-} will recombine and form S₂O₈²⁻. On the other hand, in reactors without membrane and H⁺ and OH⁻ equilibrium, the main pathway to generate SO₄^{•-} will more likely be associated to direct oxidation.

Hence, more than 80% of ATN was degraded in 240 min for all conditions and something like 80% was the maximum mineralization achieved, better results than those found in the literature for EO using single compartment and similar j_{app} and Na₂SO₄ concentration [41].

As illustrated in Fig. 4 and better viewed in the curve slope presented in the insert graphics, the concentration of Na₂SO₄ also presents a role in the electrochemical reactions using DCMR. It seems that an increase in the Na₂SO₄ concentration leads to an increase in ATN degradation. In this condition, there are more SO₄^{•-} and S₂O₈²⁻ available in the bulk solution, increasing the ATN degradation, mainly at 5 mA cm⁻². On the other hand, for mineralization, the increase in the concentration of Na₂SO₄ leads to a worst result, once again the exception was at 5 mA cm⁻².

This finding can be explained by the degradation mechanism and kinetic constants. As reported in Fig. 4, the oxidation of ATN upon electrochemical reaction in DMCR is largely dependent on the j_{app} . Assuming that the mass transport coefficient is constant at a constant experimental condition, an increase in j_{app} will lead to an increase in the HO• generation, and the equation of kinetic model can be expressed as follows:

$$\frac{dC}{dt} = -k \cdot C \cdot [\text{HO}^\bullet] \quad (9)$$

where C is the ATN concentration (mM), $[\text{HO}^\bullet]$ is the concentration of hydroxyl radicals, and k is the overall reaction constant.

For a given j_{app} , the concentration of HO^\bullet will be constant (Eq. 5) and, since other active species generated (Eqs. 6 - 8) also depends of the HO^\bullet concentration, its generation can be considered constant as well.

In this situation, Eq. 9 can be rewritten as:

$$\frac{dC}{dt} = -k_{obs} \cdot C \quad (10)$$

where k_{obs} is the pseudo-first-order reaction constant.

In all cases the degradation and mineralization profiles fit well a pseudo-first-order model for the time interval depicted in the graphics (Fig. 4). It is possible to see in the insert graphic at Fig. 4 that an increase in the j_{app} leads to a higher k_{obs} values. Nevertheless, the increase in the Na_2SO_4 concentration from 0.014 to 0.056 M shows a different behavior for the k_{obs} for the ATN degradation and mineralization.

Although the increase in Na_2SO_4 concentration exhibited a slight increase in k_{obs} values for ATN degradation, the slope of the straight-line in the inserted graphics for mineralization shows a reduction in the kinetic constant values.

This fact can be explained, considering that the application of DCMR in the electrochemical process makes the main route of ATN oxidation to be via $\text{SO}_4^{\bullet-}$ and $\text{S}_2\text{O}_8^{2-}$, as presented on the chemical equilibrium diagrams (Fig. S1, supplementary material) and at Eq. 6 - 8, as previously explained. Besides that, the rate limiting step for $\text{SO}_4^{\bullet-}$ and $\text{S}_2\text{O}_8^{2-}$ production, and consequently high ATN oxidation, is the HO^\bullet generation, which is associated to the j_{app} and Na_2SO_4 concentration. High concentrations of Na_2SO_4 , which are not reduced at the cathode due to the addition of the cationic membrane, will hinder ATN mineralization due to the competition for HO^\bullet , acting as a scavenger. In this situation, as it was already reported on Fig. 4, Na_2SO_4 concentration will play a less important role in ATN mineralization, the opposite of what was found in another work operating a single compartment reactor [41], and showed in the main effect plots (Fig. S2, supplementary material).

A study conducted by da Silva et al. [56], also demonstrated that, in single compartment reactor, the increase in the concentration of Na_2SO_4 and in the j_{app} leads to a high degradation of EOM. However, this

increase in the kinetics are not related to the complete mineralization, conducting to a high generation of transformation products [26,58,59].

Some ATN transformation products have already been described in the literature for single compartment reactors [40,60]. It was found that the operating conditions, mainly the j_{app} , affect the ATN transformation products, being the denitrification a crucial role. When high j_{app} are used, the formation of $S_2O_8^{2-}$ and $SO_4^{\bullet-}$ was benefited. They attack the N-terminal groups of ATN molecule by electron transfer reaction, leading to a fast oxidation to NO_3^- . In this case, the transformation products can be 4-Ethoxy ethylbenzoate, 4-Hydroxybenzaldehyde, Phthalic acid and Benzoic acid, methyl ester.

On the other hand, at low j_{app} , the oxidation is mainly by HO^{\bullet} abstracting protons from ATN molecule. In this case, the transformation products have N-terminal groups as 2,4-Dinitrophenol and 4-hydroxy-2-nitrophenol, Benzoyl urea and Benzenamine, 4-methyl-3-nitro-.

After all assays, it was not observed any visual membrane degradation, what was already expected, since Nafion[®] – 117 membrane is chemically stable in severe work conditions [61]. In fact, TOC analysis did not show unexpected extra carbon concentration, which could be associated to the membrane degradation.

SUPPLEMENTARY MATERIAL FOR

Evaluation of an electrochemical membrane reactor for the removal of β -blocker compound from water

Alan Nelson Arenhart Heberle^{a,c}, Giulia Grimaldi Falavigna Vianna^a, Salatiel Wohlmuth da Silva^{b*},
Valentín Pérez-Herranz^c, Andréa Moura Bernardes^a

^a Universidade Federal do Rio Grande do Sul (UFRGS) – Programa de Pós-Graduação em Engenharia de Minas, Metalúrgica e de Materiais (PPGE3M), Av. Bento Gonçalves, 9500, Porto Alegre, RS, Brazil.

^b UFRGS, Instituto de Pesquisas Hidráulicas (IPH) – Programa de Pós-Graduação em Recursos Hídricos e Saneamento Ambiental, Av. Bento Gonçalves, 9500, Porto Alegre, RS, Brazil.

^c Grupo IEC, Departamento de Ingeniería Química y Nuclear, E.T.S.I. Industriales, Universitat Politècnica de València (UPV), P.O. Box 22012, E-46071, Valencia, Spain.

*Corresponding author: salatiel.silva@ufrgs.br

1 Hydra-Medusa[®] diagrams

Aiming to investigate the pathway to form $\text{SO}_4^{\bullet-}$ on DCMR and the contributions of sulfate base species and of HO^\bullet in sodium sulfate electrolyte, analyses of the sulfate speciation and chemical equilibrium diagrams (software Hydra-Medusa[®]) in different pH were proposed.

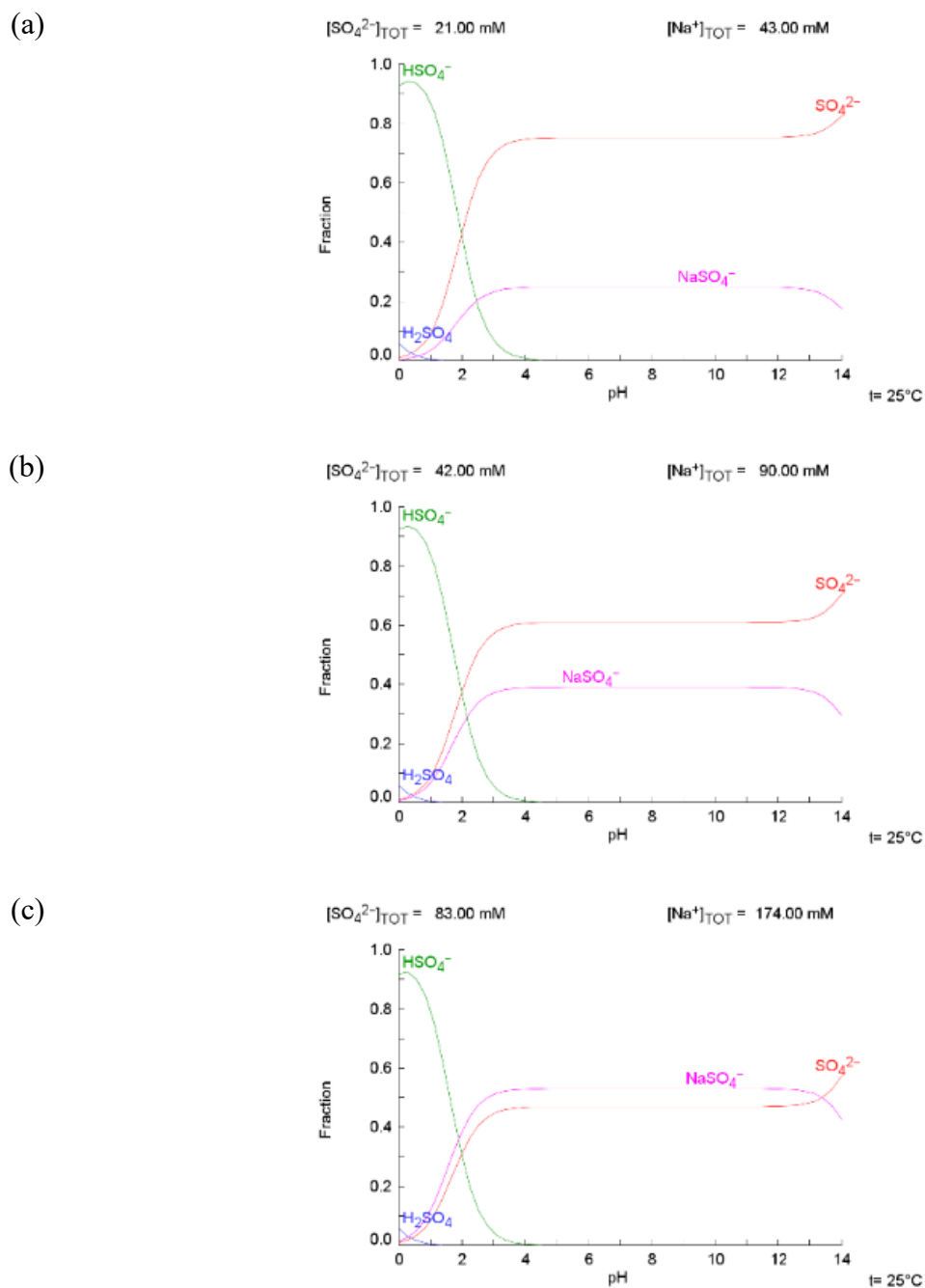


Fig. S1. Chemical equilibrium Hydra-Medusa[®] diagrams toward solutions pH and Na_2SO_4 speciation for different concentrations of Na_2SO_4 : (a) 0.014 M, (b) 0.028 M and (c) 0.056 M.

2 Effect of operating parameters on the oxidation of ATN

To evaluate the influence of the reaction time, applied current density, Na₂SO₄ concentration and reactor type on ATN oxidation, it was performed a Multilevel Factorial Design using a Minitab 17 Statistical Software, according to Table S1. In all cases the model summary has a R-sq \geq 99%.

Table S1. Parameters used for Multilevel Factorial Design

Multilevel Factorial Design

Factors:	3	Replicates:	2
Base runs:	165	Total runs:	330
Base blocks:	1	Total blocks:	1

Number of levels: 11; 5; 3

General Factorial Regression: Degradation versus t (min); i (mA cm⁻²); [Na₂SO₄]

Factor Information

Factor	Levels	Values
t (min)	11	0; 15; 30; 45; 60; 90; 120; 150; 180; 210; 240
i (mA cm ⁻²)	5	5; 10; 20; 30; 40
[Na ₂ SO ₄]	3	2; 4; 8

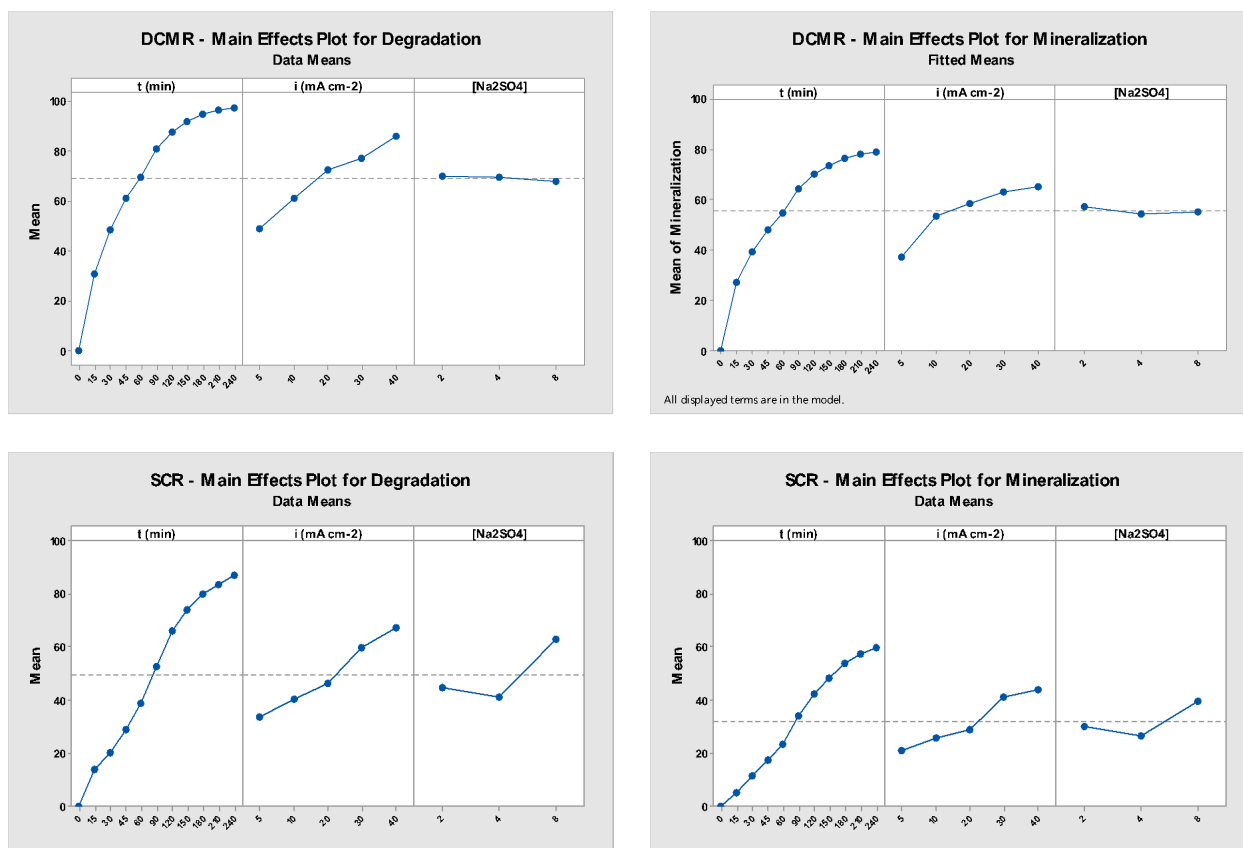


Fig. S2. Comparison of main effect plots for ATN degradation and mineralization at same electrochemical and mass transport conditions for Double Compartment Membrane Reactor (DCMR) and Single Compartment Reactor (SCR).

3 Comparison of EO process with and without membrane

3.1 Electrochemical combustion

Fig. S3 shows the estimated electrochemical combustion values vs. time, for all conditions tested in this work.

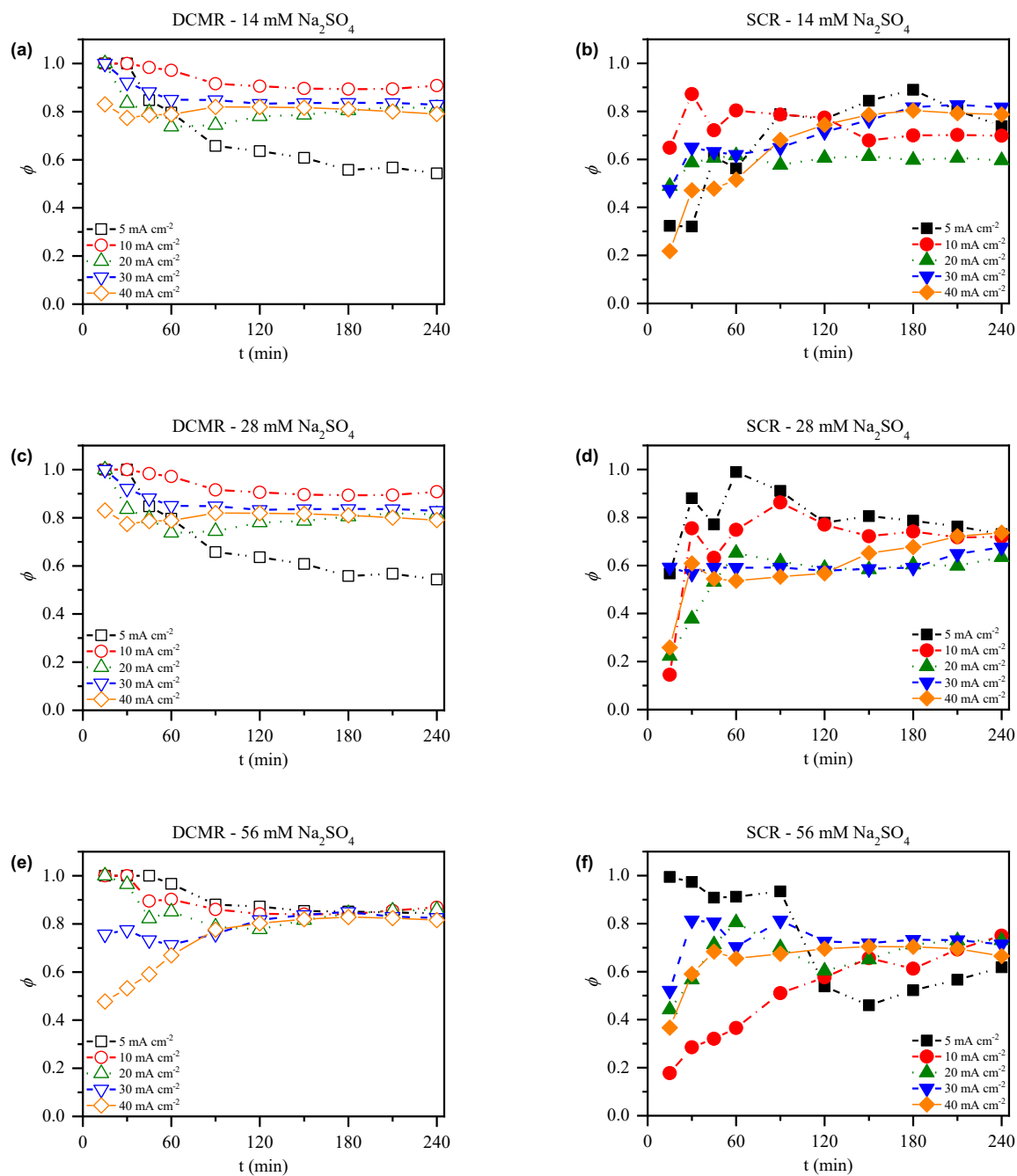


Fig. S3. Effect of the reactor configuration, current density and supporting electrolyte concentration on the electrochemical combustion. Where membrane reactor is DCMR and without membrane is SCR.

3.2 Mineralization current efficiency

Fig. S4 shows the estimated MCE values vs. time, for all conditions tested in this work.

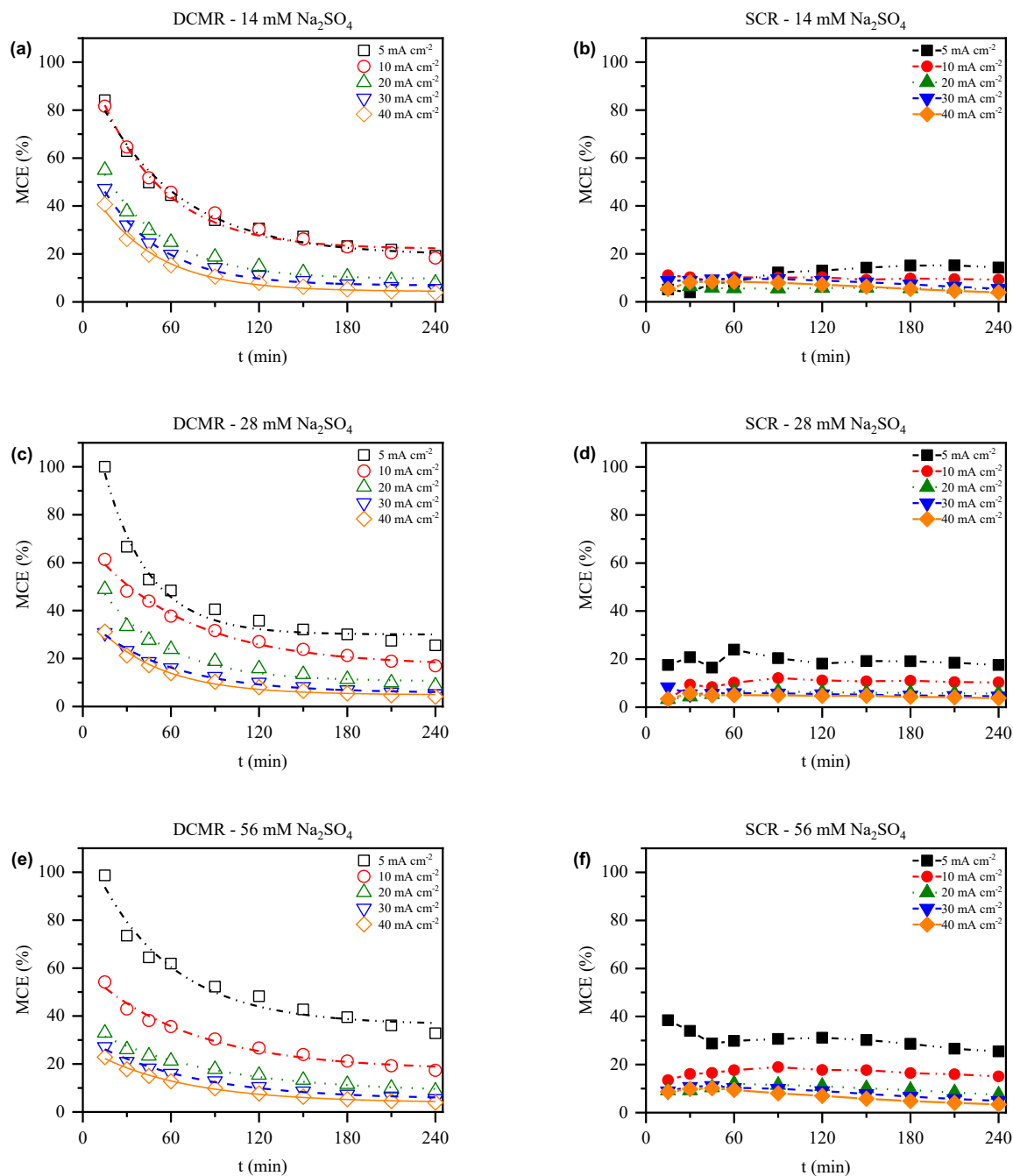


Fig. S4. Effect of the reactor configuration, current density and supporting electrolyte concentration on mineralization current efficiency. Where membrane reactor is DCMR and without membrane is SCR.

3.3 Specific energy consumption

Fig. S5 shows the estimated E_s values vs. time, for all conditions tested in this work.

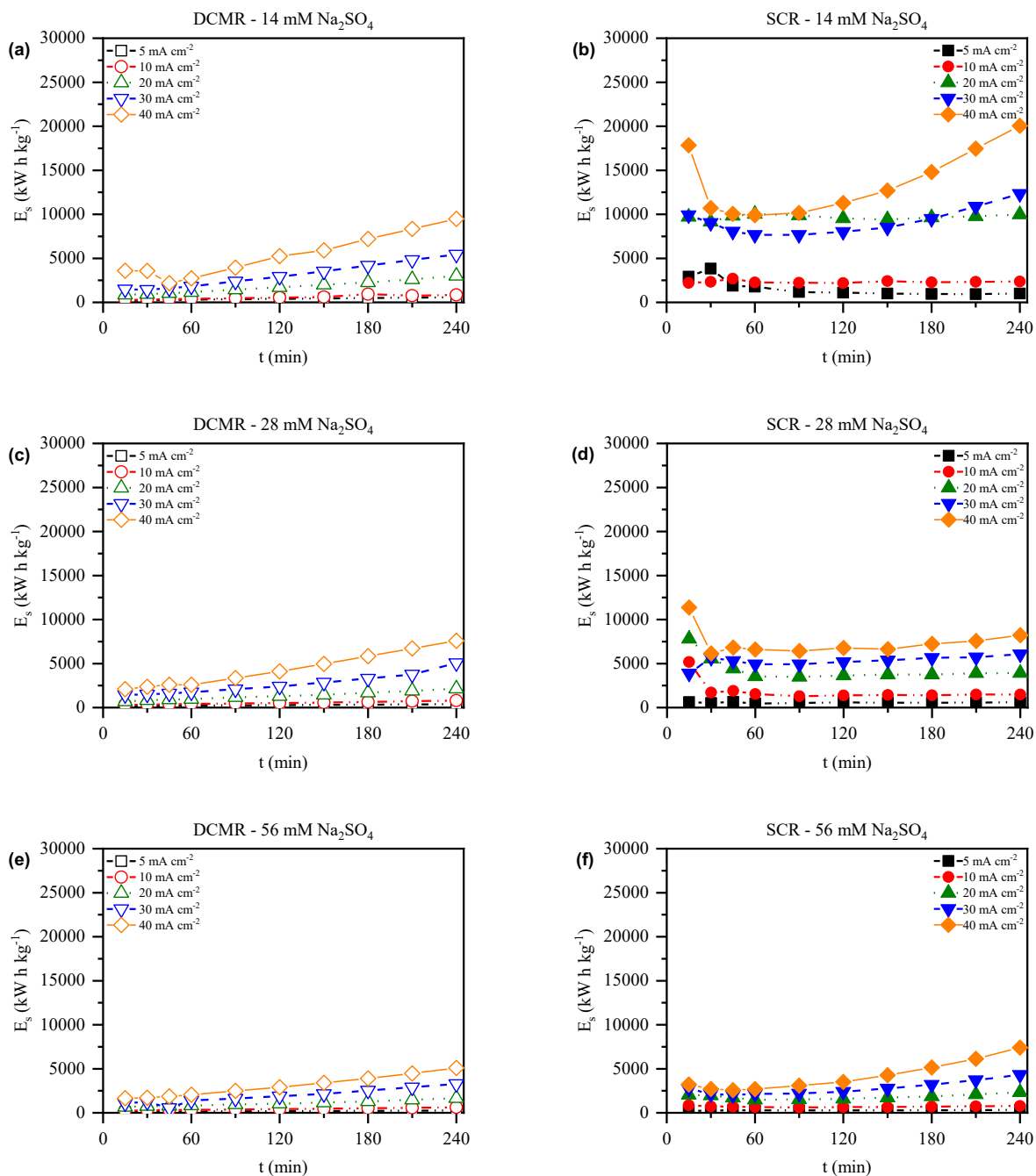


Fig. S5. Effect of the reactor configuration, current density and supporting electrolyte concentration on specific energy consumption. Where membrane reactor is DCMR and without membrane is SCR.